The Astrophysical Journal, 720:1033–1037, 2010 September 10 doi:10.1088/0004-637X/720/2/1033

EXPLORING ACCRETION AND DISK–JET CONNECTIONS IN THE LLAGN M81*

J. M. Miller[1], M. Nowak[2], S. Markoff[3], M. P. Rupen[4], and D. Maitra[1]
[1] Department of Astronomy, University of Michigan, 500 Church Street, Ann Arbor, MI 48109, USA; jonmm@umich.edu
[2] MIT Kavli Institute for Astrophysics and Space Research, 70 Vassar Street, Cambridge, MA 01239, USA
[3] Science Park 904, 1098 XH, Amsterdam NL, The Netherlands
[4] National Radio Astronomy Observatory, 1003 Lopezville Road, Socorro, NM 87801, USA
Received 2010 January 11; accepted 2010 June 28; published 2010 August 16

ABSTRACT

We report on a year-long effort to monitor the central supermassive black hole in M81 in the X-ray and radio bands. Using *Chandra* and the Very Large Array, we obtained quasi-simultaneous observations of M81* on seven occasions during 2006. The X-ray and radio luminosity of M81* are not strongly correlated on the approximately 20 day sampling timescale of our observations, which is commensurate with viscous timescales in the inner flow and orbital timescales in a radially truncated disk. This suggests that short-term variations in black hole activity may not be rigidly governed by the "fundamental plane," but rather adhere to the plane in a time-averaged sense. Fits to the X-ray spectra of M81* with bremsstrahlung models give temperatures that are inconsistent with the outer regions of very simple advection-dominated inflows. However, our results are consistent with the X-ray emission originating in a transition region where a truncated disk and advective flow may overlap. We discuss our results in the context of models for black holes accreting at small fractions of their Eddington limit and the fundamental plane of black hole accretion.

Key words: accretion, accretion disks – black hole physics – galaxies: active – galaxies: jets

1. INTRODUCTION

Low-luminosity active galactic nuclei (LLAGNs) are potentially important transition objects, harboring supermassive black holes that accrete at a rate that is intermediate between Seyfert AGNs and quasars, and extremely under-luminous sources such as Sgr A*. LLAGNs may provide clues to jet production: in these systems, compact relativistic radio jets are often detected (Nagar et al. 2002; Anderson & Ulvestad 2005), and the natural timescales are such that the details of jet production can be revealed. Moreover, LLAGNs are often "radio-loud" (Ho 2008), meaning that jets are an important part of the overall accretion flow. At a distance of only 3.6 Mpc (Freedman et al. 1994), the accreting supermassive black hole at the center of M81 powers the nearest LLAGN, M81*.

The nature of the innermost accretion flow in LLAGNs is not clear. It is likely that these sources are still fueled partially by an accretion disk—double-peaked optical emission lines are seen in M81* (Bower et al. 1996; also see Devereux & Shearer 2007)—but relativistic X-ray lines from the inner accretion disk are not clearly detected in these systems (e.g., Dewangan et al. 2004; Reynolds et al. 2009; for a review, see Miller 2007). The inner disk may be truncated, and the innermost flow may be advection-dominated (Narayan & Yi 1994; also see Blandford & Begelman 1999). Theoretical work suggests that thick advective disks and radial flows may help to maintain poloidal magnetic fields and power jets (e.g., Livio 2000; Meier 2001; Reynolds et al. 2006). X-ray observations can test and refine models for advective inflow at low mass accretion rates in a variety of ways. For instance, the inner accretion flow is predicted to be extremely hot, with temperatures ranging between 10^{12} K centrally and 10^{9}–10^{10} K in their outermost radii (Narayan & Yi 1994, 1995). Recent observations of X-ray binaries have achieved the sensitivity required to test these predictions (e.g., Bradley et al. 2007) and find emission consistent with much lower temperatures.

X-ray emission is often used as a trace of the accretion inflow (although some X-ray emission could originate in a jet; e.g., Markoff et al. 2001; also see Miller et al. 2002; Russell et al. 2010), and radio emission is used to trace the jet power. In X-ray binaries, X-ray and radio emission follow the relationship $L_R \propto L_X^{0.7}$, both in ensemble and in individual sources (Gallo et al. 2003; however, see Jonker et al. 2010). This relation has been generalized into a fundamental plane of black hole accretion, combining radio luminosity, X-ray luminosity, and black hole mass (Merloni et al. 2003; Falcke et al. 2004; Gultekin et al. 2009). If accretion physics scales predictably with black hole mass, then for any individual object of known mass, the relationship between radio and X-ray emission should be fixed, on average.

Prior to discrete jet ejection events in stellar-mass black holes, quasi-periodic oscillations (QPOs) are often observed in the X-ray flux, with a characteristic frequency of ∼6 Hz (see, e.g., Nespoli et al. 2003; Ferreira et al. 2006; Klein-Wolt & van der Klis 2008; Fender et al. 2009). If this frequency is a Keplerian orbital frequency, it corresponds to a radius of $66\,GM/c^2$ for a black hole with a mass of $10\,M_\odot$. This radius is broadly consistent with lower limits on the inner edge of the accretion disk in M81* based on the width of the Fe Kα emission line (Dewangan et al. 2004; Young et al. 2007). In stellar-mass systems, it is not possible to test disk–jet connections on the period defined by the QPO, although the oscillation might be tied to jet production. In supermassive black holes, however, this timescale is accessible. For a black hole with a mass of $7 \times 10^7\,M_\odot$ like that in M81* (Devereux et al. 2003), monitoring every 2–4 weeks can sample the corresponding timescale.

In this paper, we present contemporaneous X-ray and radio observations of M81* made using *Chandra* and the Very Large Array (VLA), with visits separated by approximately 20 days. The observations and data reduction methods are described in Section 2. Our analysis and results are presented in Section 3. We do not find a clear correlation between radio and X-ray emission

Table 1
X-ray and Radio Observations

Obs.	T_X (MJD)	Exposure (ks)	Γ	F_X (10^{-11} erg cm^{-2} s^{-1})	T_R (MJD)	Exposure (ks)	$S_{8.4}$ (mJy)	Configuration
1	53774.9	15.0	1.7(1)	1.6(1)	53775.3	3.4	110.5(1)	A
2	53800.0	15.0	1.8(1)	1.7(1)	53800.9	5.3	96.4(1)	A
3	53826.4	15.0	1.8(1)	1.6(1)	...	...	...	...
4	53849.5	14.7	1.8(1)	1.6(1)	...	...	...	...
5	53869.5	15.0	1.8(1)	1.7(1)	...	...	...	...
6	53895.8	15.0	1.8(1)	1.5(1)	53892.0	5.2	103.0(1)	A
7	53915.0	14.9	1.9(1)	1.7(1)	53915.9	5.3	81.2(1)	B
8	53929.6	15.1	1.8(1)	1.8(1)	53928.0	5.2	104.7(1)	B
9	53944.5	14.6	1.70(7)	3.1(1)	53944.7	6.3	124.0(1)	B
10	53959.7	15.0	1.70(7)	2.8(1)	53959.7	5.2	102.4(1)	B

Notes. The table lists observation times and properties of the flux observed from M81* through our joint monitoring program. The X-ray spectra were fit with simple absorbed power-law models; the power-law index and resulting 0.5–10.0 kV flux are reported above. The radio flux density at 8.4 GHz is reported from each successful observation with the VLA. All errors are 1σ confidence errors; numbers in parentheses indicate the error in the last digit.

in M81*, though a small number of simultaneous points were obtained and span a factor of approximately 2 in X-ray flux. These results are discussed in Section 4.

2. OBSERVATIONS AND DATA REDUCTION

We observed M81* on 10 occasions using *Chandra*. Each observation achieved a total exposure of approximately 15 ks (see Table 1). In order to minimize photon pile-up in the zeroth-order ACIS image, the HETGS was inserted into the light path in each case. The ACIS chips were operated in "FAINT" mode.

We used CIAO version 4.0.2 in processing the *Chandra* data. The first-order dispersed spectra from the medium energy grating (MEG) and high energy grating (HEG) were split from the standard "pha2" file, and associated instrument response files were constructed. The first-order MEG spectra and responses were then added using the CIAO tool "add_grating_spectra;" the first-order HEG spectra and responses were added in the same way. The zeroth-order ACIS spectra and responses were generated using the CIAO tool "psextract." In each case, a circular region was used to extract the source flux and a radially offset annular region was used to extract the background flux. All spectra were grouped to require at least 20 counts per bin using the FTOOL "grppha," in order to ensure the validity of χ^2 statistics.

The VLA also observed M81* on 10 occasions (see Table 1). Useful data were obtained on seven occasions that coincide with the *Chandra* X-ray observations. All observations were obtained at 8.4 GHz. The first three coincident exposures were obtained in the "A" configuration (achieving a typical angular resolution of approximately $0\farcs3$), while the last four were obtained in the "B" configuration (achieving a typical angular resolution of approximately $1''$). Standard compact calibrator sources were used to calibrate phase and amplitude variations and to set the overall amplitude scale. The average flux density measured in each exposure is reported in Table 1.

3. ANALYSIS AND RESULTS

The *Chandra* X-ray spectra were analyzed using XSPEC version 12.4 (Arnaud 1996). Spectral fits were made in the 0.5–10.0 keV band. All of the errors reported in this work are 1σ confidence errors. In calculating luminosity values, distances

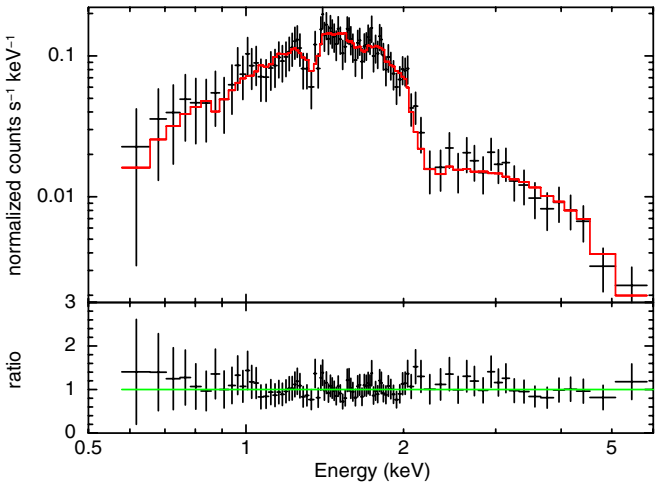

Figure 1. Plot shows the combined MEG spectrum of M81* obtained on MJD 53944. The data are acceptably fit using a simple power-law function with a photon index of $\Gamma = 1.70 \pm 0.07$ (shown in red). The lower panel shows the ratio of the observed spectrum to the power-law model.

were assumed to be absolute, and uncertainties in luminosity were derived from the flux uncertainties.

We initially made separate fits to the zeroth order, combined MEG, and combined HEG spectra. In all direct fits, the equivalent neutral hydrogen column density drifted toward zero, which is unphysical. A value of 4.1×10^{20} cm^{-2} is expected along this line of sight (Dickey & Lockman 1990), but this value is too low to be constrained directly in the MEG spectra obtained. For consistency, then, the expected value was fixed in all fits. All of the spectra were acceptably fit ($\chi^2/\nu \leqslant 1.0$, where ν is the number of degrees of freedom in the fit) with a simple power-law model (see Figure 1). The spectrum of M81* is likely more complex, mostly owing to local diffuse emission (Young et al. 2007), but a simple power law is an acceptable fit to the modest spectra obtained in our observations.

The zeroth-order spectra suffer from photon pile-up and are not robust. Particularly, in the last two *Chandra* observations, where the flux is higher, the best-fit power-law photon index was found to be harder. This is consistent with multiple low-energy X-rays being detected as single high energy photons. Moreover, the data/model ratio in each spectrum shows an increasing positive trend with energy. The HEG spectra contain

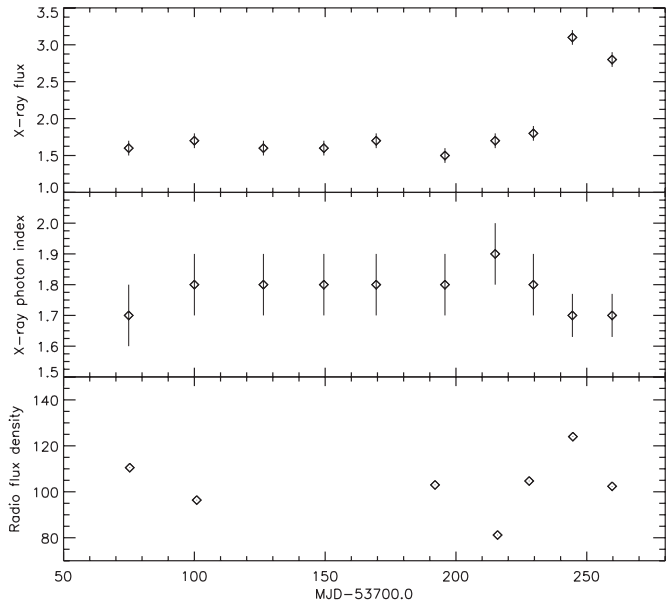

Figure 2. Plot shows the evolution of 0.5–10.0 keV X-ray flux, X-ray photon index, and 8.4 GHz radio flux density observed in M81* with time. The X-ray flux is plotted in units of 10^{-11} erg cm^{-2} s^{-1}. The radio flux density is plotted in units of 100 mJy. The errors shown on all quantities are 1σ errors; the flux density errors are smaller than the plotting symbols.

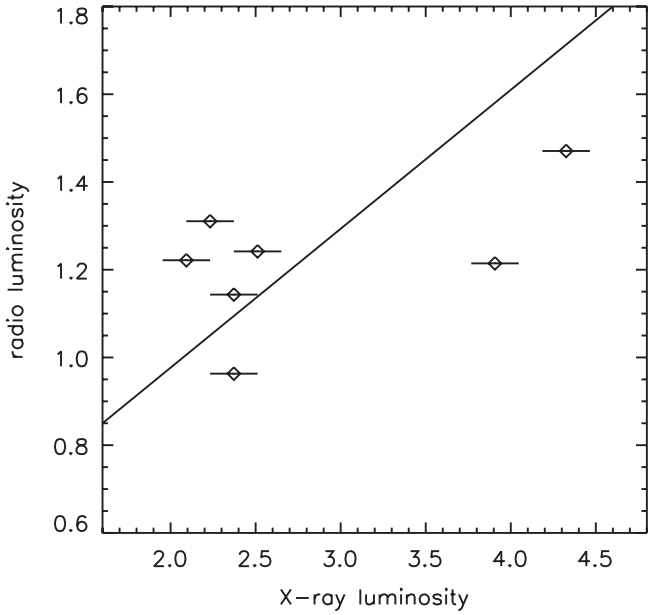

Figure 3. 8.4 GHz radio luminosity of M81* (in units of 10^{37} erg s^{-1}) is plotted against its 0.3–10.0 keV X-ray flux (in units of 10^{40} erg s^{-1}) in the figure. The errors shown are 1σ errors; the error on radio luminosity is very small. In spectrally hard black hole sources with jets, an $L_R \propto L_X^{0.7}$ is expected. The solid line above plots $L_R = C \times L_X^{0.7}$, where $C = 6 \times 10^8$ was chosen arbitrarily. The X-ray and radio luminosity values are not significantly correlated.

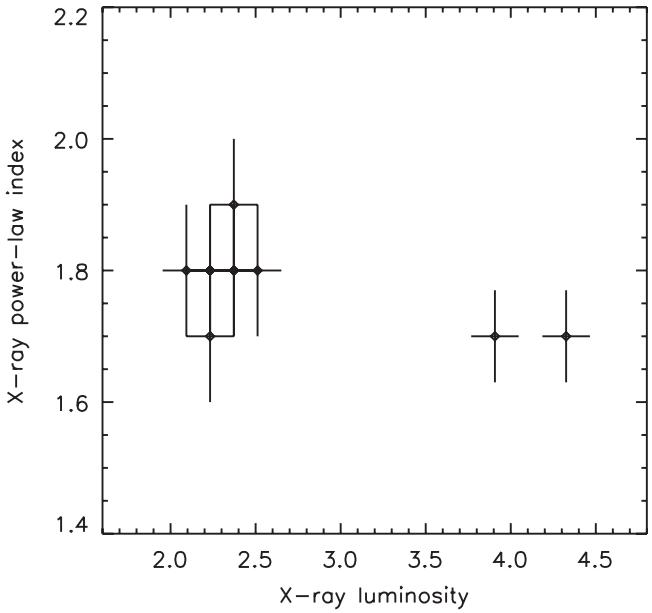

Figure 4. X-ray photon power-law index is plotted vs. the 0.3–10.0 keV X-ray luminosity of M81* (in units of 10^{40} erg s^{-1}) in the figure. There is no evidence of the correlations observed in Seyferts and stellar-mass black holes, though a relatively small range in luminosity and spectral index is sampled in our observations.

many fewer photons than the MEG spectra and were found to be of little help in constraining the source flux or spectral index. We therefore restricted our flux analysis to the combined first-order MEG spectra. The second spectrum listed in Table 1, for instance, has just over 2800 photons, and the penultimate spectrum has 4900 photons.

The results of our spectral analysis of each observation are detailed in Table 1. Figure 2 shows the time evolution of the X-ray flux, X-ray power-law photon index, and radio flux density. Between MJD 53900.0 and MJD 53950.0, the X-ray flux increases by a factor of approximately 2, and the radio flux density increases by slightly less than a factor of 2. The X-ray spectral index does not vary significantly during the course of our observations. In each spectrum, the index is consistent with $\Gamma = 1.7$, which is fairly typical of Seyferts (see, e.g., Reynolds 1997) and consistent with prior *Chandra* observations of M81* (Young et al. 2007). A power law is not a unique description of the data; bremsstrahlung models also yield acceptable fits with temperatures of $kT = 5 \pm 2$ keV.

Assuming a flat radio spectrum, we calculated the radio luminosity in the narrow VLA band centered at 8.4 GHz. We also calculated the unabsorbed X-ray flux in the 0.5–10.0 keV band. We assumed a distance of 3.6 Mpc to M81* (Freedman et al. 1994). This radio luminosity is plotted versus the X-ray luminosity in Figure 3. The Spearman's rank correlation coefficient for the flux values is 0.23, and it is apparent in Figure 3 that there is no strong correlation between the X-ray and radio luminosity.

In Figure 4, the X-ray power-law photon index is plotted versus the X-ray luminosity. Here again, there is no clear correlation visible in the plot. The Spearman's rank correlation coefficient for these quantities is -0.39, indicating that there is no significant correlation.

The sampling rate of the X-ray light curve is 21 ± 5 days and that of the radio light curve is 19 ± 5 days. Therefore, the radio and X-ray peak around MJD 53944.6 are formally consistent with being simultaneous, and any delay between radio and X-rays is $\leqslant$20 days. Given the sampling rate, it is likely that the radio/X-ray flare is caused by a factor of $\sim$2 change in $\dot{M}$ between MJD 53929 and 53960.

4. DISCUSSION AND CONCLUSIONS

The nature of the inner accretion flow in LLAGNs is not yet clear. It is possible that LLAGNs retain many of the characteristics of Seyferts, perhaps including an accretion disk extending to the ISCO (e.g., Herrnstein et al. 1998; Maoz 2007). It is also possible that LLAGNs are more like under-luminous

sources, such as Sgr A*, and best described in terms of an ADAF or coupled ADAF–jet system (see, e.g., Nemmen et al. 2010). In this work, we have attempted to explore the nature of the inner accretion flow in an LLAGN by examining evidence for a disk–jet connection in M81*. Based on observations of QPOs with a frequency of ∼6 Hz in stellar-mass black holes just prior to jet ejection episodes, we sampled a commensurate timescale in M81*. If this timescale is an orbital period, it implies a radius that is compatible with lower limits on the inner radius of the accretion disk in M81* based on the modeling of the Fe Kα emission line detected in deep observations of this source ($R \geqslant 50$–$60\ GM/c^2$; Dewangan et al. 2004; Young et al. 2007). If the innermost accretion flow is advective, so that it is geometrically thick but retains some viscosity and angular momentum, then our sampling timescale is also commensurate with the viscous timescale in the very innermost region around the black hole (e.g., $6\ GM/c^2$). Our monitoring observations improve upon many prior investigations of disk–jet connections in many supermassive and stellar-mass black holes in that our radio and X-ray observations were nearly simultaneous.

At low fractions of the Eddington limit, stellar-mass black holes have hard X-ray spectra (see, e.g., Miller et al. 2006; Miller et al. 2006; Tomsick et al. 2008; Reis et al. 2010; for a review, see Remillard & McClintock 2006) and radio emission that is consistent with a compact jet (Fender et al. 2009). Both in individual sources and in an ensemble, radio and X-ray emission are related by the expression $L_R \propto L_X^{0.7}$ (Gallo et al. 2003; see, however, Jonker et al. 2010).

Our data neither strongly confirm nor reject the possibility that M81* regulates its radio and X-ray output according to $L_R \propto L_X^{0.7}$ (see Figure 3). However, it is clear that if M81* does follow this relation, the regulation of its radiation is not rigid on short timescales. Recent work on Sgr A* shows that the source approaches the expected relation when it flares, but otherwise falls below it (Markoff 2005). These outcomes suggest that black holes might generally channel a fixed fraction of the matter inflow (traced by X-ray emission) into a jet (traced by radio emission), but not necessarily at every moment. Said differently: the energy channeled into jets at any given time may vary as it is likely to be somewhat stochastic, but on average the expected relationship may hold. In past investigations, scatter in the $L_R \propto L_X^{0.7}$ relation and the fundamental plane (e.g., Gultekin et al. 2009) could plausibly be explained in terms of non-simultaneous X-ray and radio observations; our results suggest a degree of intrinsic scatter.

Within states where compact, steady jets are produced, spectral hardness and luminosity are positively correlated in stellar-mass black holes (e.g., Tomsick et al. 2001; also see Rykoff et al. 2007). Hardening of this kind has also been observed in Sgr A* (Baganoff et al. 2001). In contrast, Seyferts appear to become spectrally softer with higher X-ray luminosity (see Vaughan & Fabian 2004). The X-ray spectrum of M81* does not show a strong trend with luminosity, and we are not able to characterize the variability of M81* as being more like Sgr A* or more typical of Seyferts.

Recent modeling of the broadband spectrum of M81* suggests that its accretion flow may be very similar to that in the hard state of stellar-mass black holes and Sgr A*. Markoff et al. (2008) showed that the same jet-dominated broadband accretion flow model can be applied to stellar-mass black holes, Sgr A*, and to M81*. The stellar-mass black hole V404 Cyg may be the source in which X-ray observations permit the best constraints on the inner accretion flow at $10^{-5}\ L_{\rm Edd.}$. Recent analysis by Bradley et al. (2007) measures a temperature of $kT \simeq 5$ keV with bremsstrahlung models. This is much too cold for even the outer parts of a simple advection-dominated accretion flow, for which temperatures of $kT \geqslant 85$ keV are predicted (Narayan & Yi 1995). Similarly, fits to our spectra of M81* with bremsstrahlung models give $kT = 5 \pm 2$ keV. In this sense, then, the X-ray spectrum of M81* is inconsistent with very simple ADAF models because a ∼5 keV plasma is too cold to be compatible with such models.

On the other hand, Young et al. (2007) showed that a combined 282 ks *Chandra* spectrum of M81* (essentially at the flux level of the first eight observations presented here) could be described by a model that was dominated by emission from collisional plasma with temperatures ranging from 1 to 100 keV. In terms of an emission measure analysis, the peak emission came from ≈10 to 30 keV plasma. Similarly, one could construct an ADAF-type model where $kT \propto R^{-0.5}$, with emission ranging from ≈1 to $10^4\ GM/c^2$. The construction of such models, however, relied upon the detection and measurement of plasma emission line features, which are too weak to detect in any of our short, individual observations. (We have verified, however, that the basic line structure reported by Young et al. is unaltered in the full, combined 450 ks spectra.) In principle, if one could associate line variations with the factor >2 continuum flux level variations shown here, especially for the lower temperature lines that should arise in the less central parts of the system, this would place strong constraints on any ADAF-type model.

The large increase in X-ray flux detected in our last two observations occurred on a timescale shorter than two weeks, which corresponds to a light travel distance of $\approx 10^{3.5}\ GM/c^2$. This is smaller than the ADAF emission region postulated by Young et al. (2007), which in any case would respond on timescales longer than the light travel time. Thus, any correlated line/continuum changes would alter the simple ADAF assumptions of emission dominated by a hot, optically thin, flow. For example, in a situation where the hot inner flow and thin disk partially overlap, a transition region with a lower temperature may be expected. Transition regions have been treated in some detail in numerous works, including Blandford & Begelman (1999) and Meyer et al. (2000). Emission originating in a transition region can potentially explain our spectral and variability results and those reported by Young et al. (2007). Moreover, this possibility is qualitatively consistent with evidence of thin disks extending to small radii at low Eddington fractions in LLAGNs and LINERS (Maoz 2007) but still allows for a coupled ADAF plus jet system like that described by Nemmen et al. (2010).

Decisive observations may be feasible with the proposed *International X-ray Observatory* (*IXO*): a single 30 ks observation with *IXO* will achieve a sensitivity greater than that in the combined 282 ks *Chandra* exposure analyzed by Young et al. (2007). The higher spectral resolution of the calorimeter expected to fly aboard *IXO* will facilitate both the detection of weak lines and the detection of small velocity shifts. If the innermost accretion flow in M81* is a dynamic environment where X-ray flares help to drive a jet and/or a wind, *IXO* spectroscopy will be able to detect corresponding variations in the line spectrum discussed by Young et al. (2007). If a weak iron line is produced in the inner disk, the sensitivity of *IXO* will help to detect and resolve the dynamical information imprinted on any such line.

We thank the anonymous referee for thoughtful comments that improved this paper. J.M.M. gratefully acknowledges

funding from the *Chandra* Guest Observer program. S.M. gratefully acknowledges support from a Netherlands Organization for Scientific Research (NWO) Vidi Fellowship. We thank the *Chandra* and VLA observatory staff for executing this demanding program.

REFERENCES

Anderson, J. M., & Ulvestad, J. S. 2005, ApJ, 627, 674
Arnaud, K. A. 1996, in ASP Conf. Ser. 101, Astronomical Data Analysis Software and Systems V, ed. G. H. Jacoby & J. Barnes (San Francisco, CA: ASP), 17
Baganoff, F., et al. 2001, Nature, 413, 45
Blandford, R. D., & Begalman, M. C. 1999, MNRAS, 303, L1
Bower, G., et al. 1996, AJ, 111, 1901
Bradley, C., et al. 2007, ApJ, 667, 427
Devereux, N., & Shearer, A. 2007, ApJ, 671, 118
Devereux, N., et al. 2003, AJ, 125, 1226
Dewangan, G., Griffiths, R. E., Di Matteo, T., & Schurch, N. J. 2004, ApJ, 607, 788
Dickey, J. M., & Lockman, F. J. 1990, ARA&A, 28, 215
Falcke, H., Kording, E., & Markoff, S. 2004, A&A, 414, 895
Fender, R., Homan, J., & Belloni, T. 2009, MNRAS, 396, 1370
Ferreira, J., et al. 2006, A&A, 447, 813
Freedman, W. L., et al. 1994, ApJ, 427, 628
Gallo, E., Fender, R. P., & Pooley, G. G. 2003, MNRAS, 344, 60
Gultekin, K., Cackett, E. M., Miller, J. M., Di Matteo, T., Markoff, S., & Richstone, D. O. 2009, ApJ, 706, 404
Herrnstein, J. R., et al. 1998, ApJ, 497, L69
Ho, L. C. 2008, ARA&A, 46, 475
Jonker, P. G., et al. 2010, MNRAS, 401, 1255
Klein-Wolt, M., & van der Klis, M. 2008, ApJ, 675, 1407
Livio, M. 2000, AIP Conf. Proc. 522, Cosmic Explosions: Tenth Astrophysics Conference, ed. W. W. Zhang & S. S. Holt (Melville, NY: AIP), 275
Maoz, D. 2007, MNRAS, 377, 1696
Markoff, S. 2005, ApJ, 618, L103
Markoff, S., Falcke, H., & Fender, R. 2001, A&A, 372, L25
Markoff, S., et al. 2008, ApJ, 681, 905
Meier, D. 2001, Astrophys. Space Sci. Suppl., 276, 245
Merloni, A., Heinz, S., & Di Matteo, T. 2003, MNRAS, 345, 1057
Meyer, F., Liu, B. F., & Meyer-Hofmeister, E. 2000, A&A, 361, 175
Miller, J. M. 2007, ARA&A, 45, 441
Miller, J. M., Ballantyne, D. R., Fabian, A. C., & Lewin, W. H. G. L. 2002, MNRAS, 335, 865
Miller, J. M., Homan, J., & Miniutti, G. 2006, ApJ, 652, L113
Miller, J. M., Homan, J., Steeghs, D., Rupen, M., Hunstead, R. W., Wijnands, R., Charles, P., & Fabian, A. C. 2006, ApJ, 653, 525
Nagar, N. M., Falcke, H., Wilson, A. S., & Ulvestad, J. S. 2002, A&A, 392, 53
Narayan, R., & Yi, I. 1994, ApJ, 428, L13
Narayan, R., & Yi, I. 1995, ApJ, 452, 710
Nemmen, R. S., Storchi-Bergmann, T., Eracleous, M., & Yuan, F. 2010, in IAU Symp. 267, Co-evolution of Central Black Holes and Galaxies, ed. B. M. Peterson, R. S. Somerville, & T. Storchi-Bergmann (Cambridge: Cambridge Univ. Press), 313
Nespoli, E., et al. 2003, A&A, 413, 235
Reis, R. C., Fabian, A. C., & Miller, J. M. 2010, MNRAS, 402, 836
Remillard, R. A., & McClintock, J. E. 2006, ARA&A, 44, 49
Reynolds, C. S. 1997, MNRAS, 286, 513
Reynolds, C. S., Garofalo, D., & Begelman, M. C. 2006, ApJ, 651, 1023
Reynolds, C. S., et al. 2009, ApJ, 691, 1159
Russell, D. M., Maitra, D., Dunn, R. J. H., & Markoff, S. 2010, MNRAS, 405, 1759
Rykoff, E. S., Miller, J. M., Steeghs, D., & Torres, M. A. P. 2007, ApJ, 666, 1129
Tomsick, J., Corbel, S., & Kaaret, P. 2001, ApJ, 563, 229
Tomsick, J., et al. 2008, ApJ, 680, 593
Vaughan, S. M., & Fabian, A. C. 2004, MNRAS, 348, 1415
Young, A. J., Nowak, M., Markoff, S., Marshall, H. L., & Canizares, C. R. 2007, ApJ, 669, 830